THIS SPEC IS OBSOLETE

Spec No: 001-40920

Spec Title: SENSING: ULTRASOUND MOTION SENSOR - AN2047

Sunset Owner: M Ganesh Raaja (GRAA)

Replaced by: None

AN2047

Sensing: Ultrasound Motion Sensor

Author: Victor Kremin
Associated Project: Yes
Associated Part Family: CY8C26443
Software Version: NA
Related Application Notes: None

This application note describes an ultrasound motion detection sensor based on the Doppler-Effect. The sensor is primarily intended to be used in security systems for detection of moving objects. However, it can be effectively involved in intelligent children's toys, automatic door opening devices, and sports training and contact-less-speed measurement equipment.

OBSOLETE

Contents

Introduction 1
Overview of Ultrasound Motion Detection Sensors 2
Sensor Flowchart 3
Sensor Hardware 4
  Sensor Schematics 4
  Chip Internals 7
  Sensor Firmware 8
Design Variances and Sensor's Alternative Applications 9
Summary 12
Appendix A 13
Worldwide Sales and Design Support 16

Introduction

Modern security systems use many types of sensors to detect access attempts by unauthorized objects. The sensor collection includes infrared, microwave, and ultrasound devices that are intended to detect moving objects. Each type of sensor is characterized by its own advantages and drawbacks. Microwave sensors are effective in large apartments because microwaves pass through dielectric materials. But these sensors consist of expensive super-high frequency components, and their radiation is unhealthy for living organisms.

Infrared sensors are characterized by high sensitivity and low cost, and are widely used. But these sensors can generate false alarm signals if heating systems are active or temperature-change speed exceeds some threshold level. Moreover, infrared sensors appreciably lose sensitivity if small insects penetrate the sensor lens.

Ultrasound motion detection sensors are characterized by small power consumption, suitable cost, and high sensitivity. This is why this kind of sensor is commonly used in home, office, and car security systems. Existing ultrasound sensors consist of multiple passive and active components and are relatively complicated for production and testing. Sensors often require a laborious tuning process. The sensor proposed in this application note uses a single PSoC MCU together with few passive components. It is characterized by high sensitivity and resistance to various noise signals.

Overview of Ultrasound Motion Detection Sensors

Figure 1 depicts the typical sensor installation.

Figure 1. Basic Sensor Operation Principle

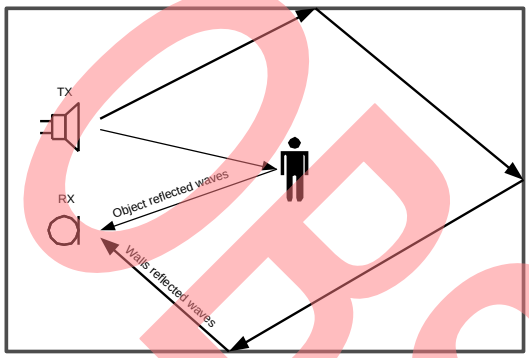

The ultrasound transmitter **TX** is emitting ultrasound waves into sensor ambient space continuously. These waves are reflecting from various objects and are reaching ultrasound receiver **RX**. There is a constant interference figure if no moving objects are in the placement.

Any moving object changes the level and phase of the reflected signal, which modifies the summed received signal level. Most low-cost sensors (car security systems, for instance) perform reflected signal amplitude analysis to detect moving objects. Despite implementation simplicity, this detection method is characterized by a high sensitivity to noise signals. For example, heterogeneous airflows, sensor vibrations, room window and door deformations, and wind gusts can change the interference figure and generate false alarm signals.

Better noise resistance may be obtained if the receive sensor is performing reflected signal frequency analysis instead of amplitude examination. The reflected signal spectrum emulates a Doppler Effect. Frequency components of the moving object speed vector have a component in the direction of ultrasound radiation propagation. Because ultrasound waves reflect from the windows, walls, furniture, and other objects, the sensor can detect object movements in any direction. To implement this principle, the sensor must perform selection and processing of Doppler Effect frequency shift to detect moving objects.

Air conditioning systems, heat generators, and refrigerators typically include movable parts, which can cause device vibrations that generate high-frequency Doppler components in the reflected ultrasound signal. The heterogeneous variable temperature airflows are characterized by different ultrasound propagation speed that can raise low-frequency Doppler components in the reflected signal. That is why the noise-resistant motion detection sensor should limit the Doppler signals' frequency range from lower and upper bounds to satisfactory false-alarm free operation.

The ultrasound motion detection sensor has been developed in compliance with operation principles described in this section. Table 1 summarizes the main sensor characteristics.

Table 1. Main Sensor Characteristics

Item	Item Value
Operation Range	5 cm–4 m
Operation Frequency	30-50 kHz, determined by piezoelectric sensor resonant frequency
Power Consumption	27 mA (alarm off) 55 mA (alarm on)
Sensor Outputs	Alarm LED and relay with normal closed and normal open contact pairs
Sensor Response Time	0.25 s
The Range of Detected Object's Speed	10 cm/s–1.5 m/s

OBSOLETE

Sensor Flowchart

The sensor flowchart is illustrated in Figure 2. Note that the gray blocks are used to mark the external units for the PSoC microcontroller.

Figure 2. Sensor Block Diagram

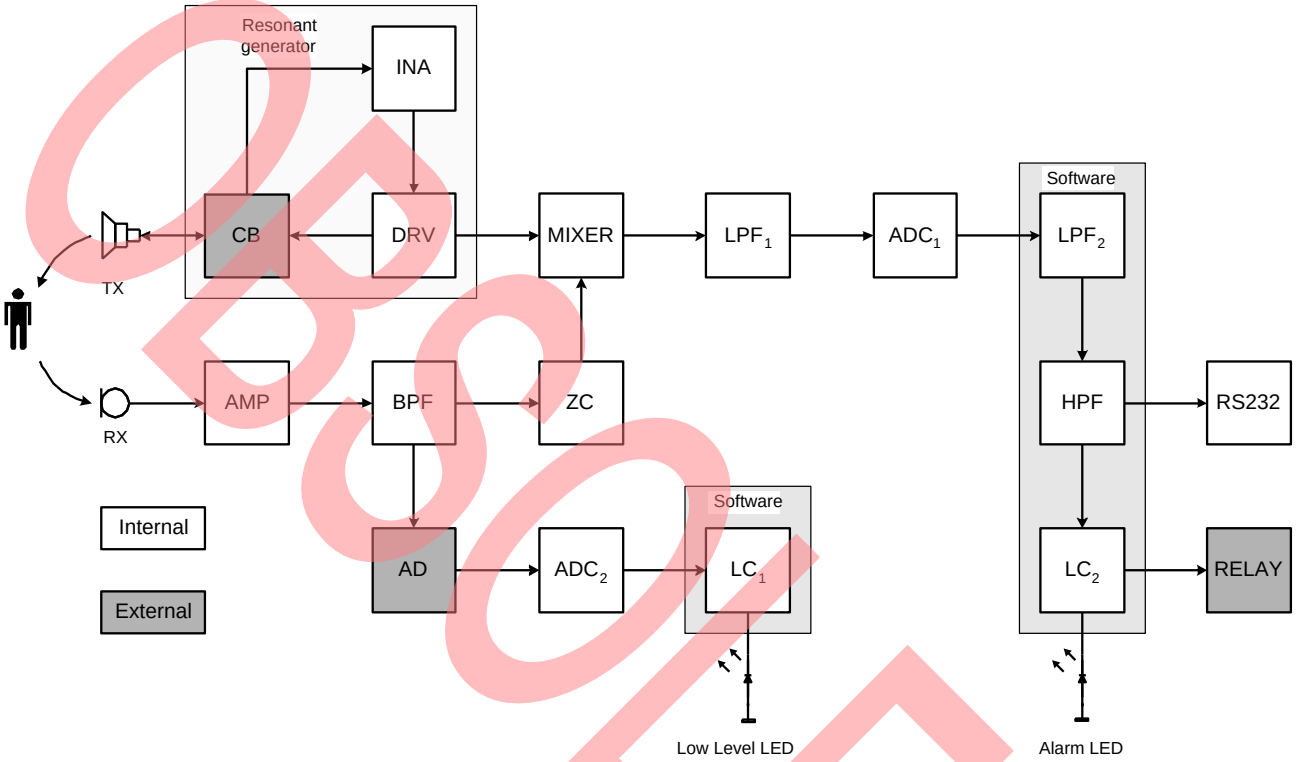

OBSOLETE

The sensor operates in the following way:

The resonant generator drives the piezoelectric transmitter **TX**, which converts the electric signals into acoustic waves. The waves reflected from various objects reach the piezoelectric receiver **RX**, are converted into electric signals and amplified by input amplifier **AMP**. The resonant band-pass filter **BPF** suppresses the off-band noise signals and removes the DC component from the input amplifier output signal.

Note The offset level of input amplifier can raise the DC component up to 0.75 V.

As considered previously, the reflected signal can be amplitude modulated. Zero-crossing detector **ZC** suppresses this unwanted amplitude modulation, and converts the filter output signal into phase modulated signal. Note that if the amplitude for the signal reflected from the moving objects is smaller than for the signal reflected from fixed items, the band-pass filter output signal will be phase modulated. It will be frequency modulated in the opposite case. In the security system, the signal reflected from moving objects can be 3 to 20 times weaker than the signal reflected from unmoved objects.

The output of zero-crossing detector **ZC** is routed to signal input of the **MIXER**. The ultrasound generator output signal serves as the **MIXER** reference signal. The low-pass filter **LPF_1** selects the Doppler signal from the mixer products. Filter output signal is then sampled by sigma-delta **ADC_1** for subsequent processing in the software. The software-implemented digital low-pass filter **LPF_2** additionally suppresses high-frequency components in Doppler signal frequency spectrum and removes the influence of zero-crossing detector phase noise.

Note In author's opinion, this noise is caused by BPF operational amplifier's noise and by PSoC digital part noise.

Digital high-pass filter **HPF** limits the lower frequency in the Doppler spectrum. It effectively suppresses the influence of low-frequency noise signals on sensor operation. The high-pass, filter-output signal is analyzed by the level comparator **LC_2** for alarm signal generation. For alternative sensor applications or testing purposes, the filtered data stream can be transmitted using an RS232 compatible transmitter.

For reliable detection of movable objects, the reflected waves' signal level must be larger than some predefined value. If this condition is not satisfactory, the sensor must be placed in another location or transmitter output power must be increased. The input level controlling subsystem consists of amplitude detector **AD**, integrating analog-to-digital converter **ADC_2** and level comparator **LC_1**.

Piezoelectric sensors are characterized by a high Q factor and need precision tuning of operation frequency to achieve the maximum efficiency. Moreover, the sensor resonant frequency is temperature dependent and influenced by aging. As a result, expensive frequency and temperature compensation circuits are present in most ultrasound sensors today. Additionally, the piezoelectric sensors need relatively large input voltages for obtaining the demanded acoustic output power. These difficulties can be eliminated if a resonant generator is used in conjunction with a piezoelectric transmitter to stimulate bridge-load driver. If the same sensor is used for the receiver part, the temperature and aging effects on sensor performance is virtually eliminated.

The proposed sensor includes the resonant generator with a bridge transmitter for achieving maximum output power for given supply voltage. This generator consists of the piezoelectric driver **DRV**, a sensor current bridge **CB** for measuring crystal current, and instrumentation amplifier **INA**.

Sensor Hardware

First, the detailed circuit diagram will be analyzed, then possible project improvements and design variations will be considered.

Sensor Schematics

Figure 3 and Figure 4 represent the complete sensor schematic. Figure 3 depicts the analog components and Figure 4 represents the CPU.

OBSOLETE

Figure 3. Sensor Schematic; Analog Components

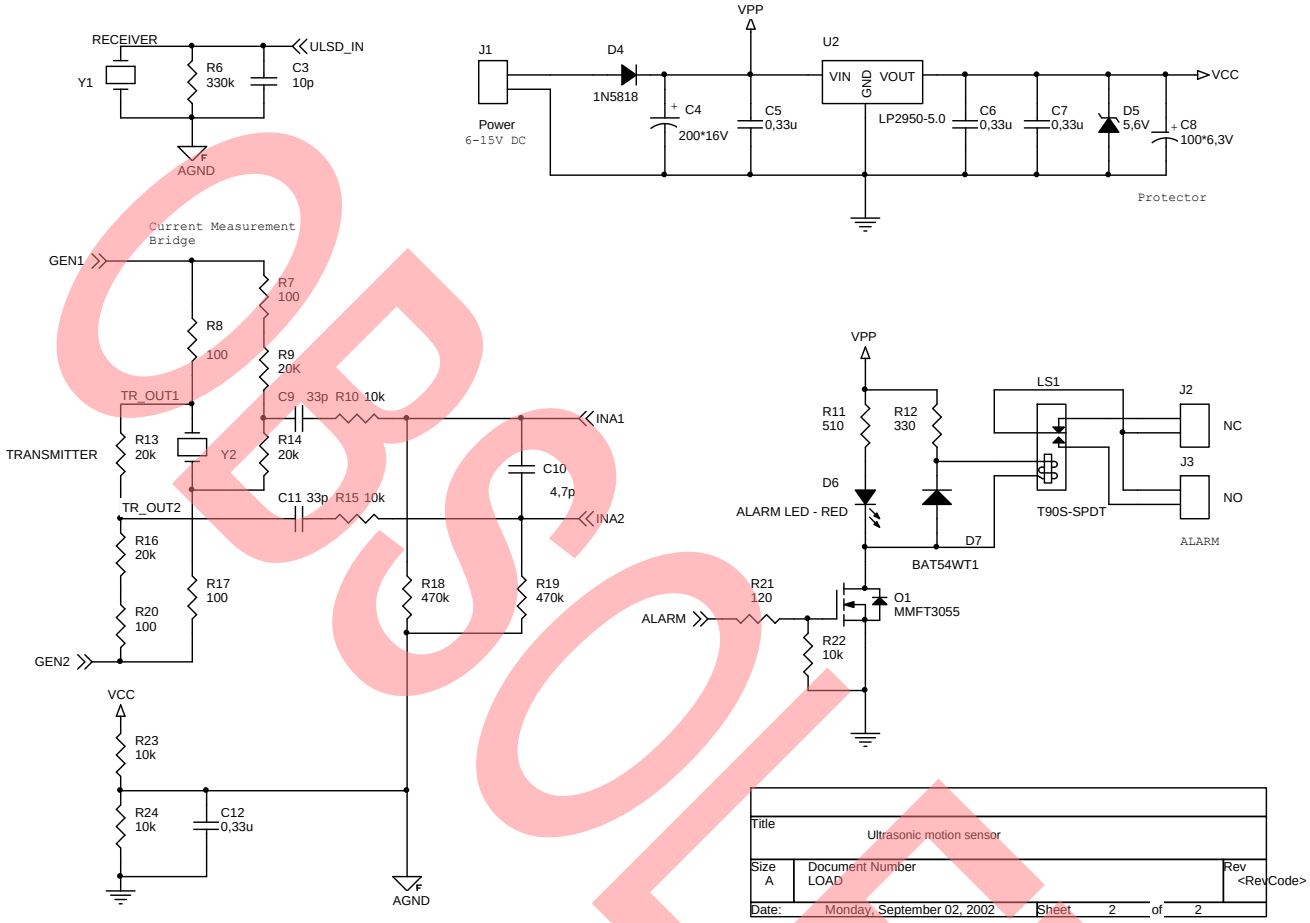

OBSOLETE

Figure 4. Sensor Schematic; CPU

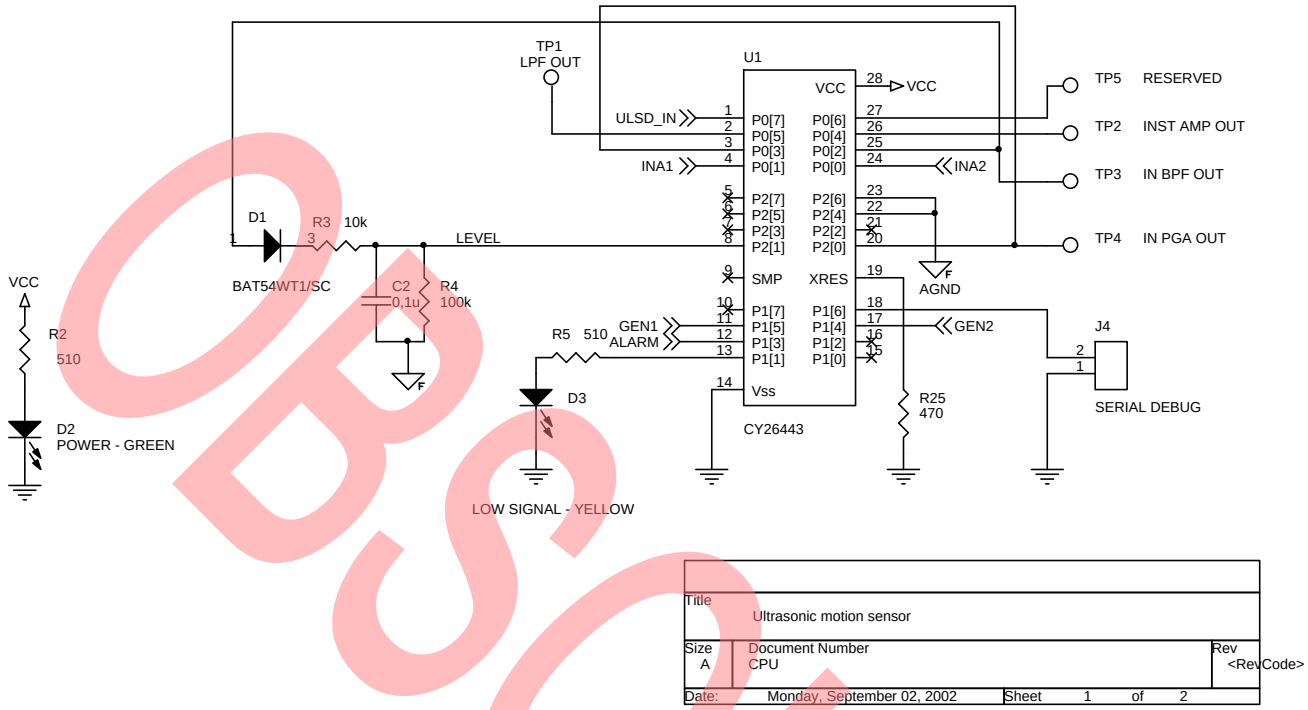

The transmitter sensor current bridge has been formed by R_7-R_9, R_{13}-R_{14}, R_{16}-R_{17} and R_{20}. If $R_8 + R_{13} = R_{16} + R_{20}$ and $R_7 + R_9 = R_{14} + R_{17}$. The voltage between the left pins of C_9 and C_{11} is directly proportional to the current in the piezoelectric transmitter Y_2. The differential networks, $C_9R_{10}R_{18}$ and $C_{11}R_{15}R_{19}$, compensate the phase shift in the internal PSoC MCU instrumentation amplifier and provide oscillation frequency very close to the main crystal resonance frequency. The network parameters are optimal for an oscillation frequency of 30-40 kHz and can be adjusted for other crystal's resonant frequencies. The sensor input stage has been formed by R_6C_3, so the $R_{23}R_{24}C_{12}$ determines the analog ground potential. The alarm relay is controlled by the Q_1 MOSFET. The other load types (such as open-drain output, solid state relay, and buzzer) can be supported as well. The power supply consists of conventional linear regulator U_2. The diode D_4 protects the sensor electronics under reverse power conditions. The sensor can be powered from non-stabilized 6-12 V DC/AC supply with maximum current of 100 mA. Normal operation current is several times smaller.

The $D_1R_3C_2R_4$ form the amplitude detector for measuring the reflected signal level. LED D_3 indicates the low level of this signal. Connector J_4 brings the compatible CMOS serial transmitter output and can be used for sensor firmware debugging or alternative sensor applications.

To send this data stream to PC COM port for analysis, a standard level translator such as MAX3221 must be added externally.

The testpoints TP_1-TP_5 are intended for observing some PSoC MCU internal signals. Table 2 describes each testpoint function:

Table 2. Testpoint Descriptions

Testpoint Reference	Function
TP1	Output of switching capacitor low-pass filter, LPF_1 according to Figure 2
TP2	Output of generator instrumentation amplifier, INA
TP3	Output of band-pass filter, BPF
TP4	Output of receiver preamplifier, AMP; input of band-pass filter, BPF
TP5	Reserved for future extensions

OBSOLETE

Chip Internals

Figure 5 shows the total chip interconnection. The port labels in brackets display the corresponding port numbers. The italic font depicts the matching net names and narrow lines have been used for presenting the clock lines. Gray color marks the unused blocks, which can be used to implement additional features.

Figure 5. PSoC MCU Internals

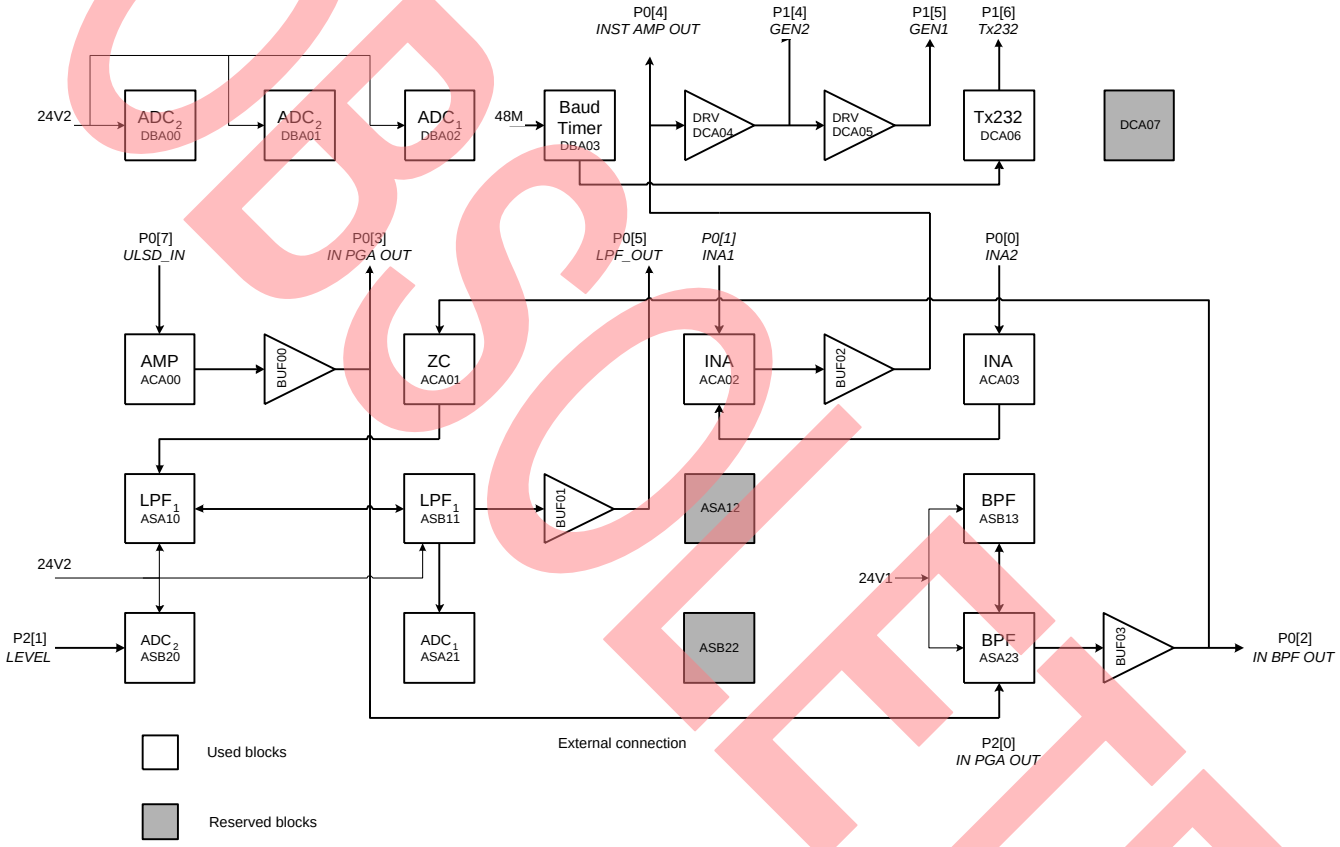

The resonant generator consists of the instrumentation amplifier, which is placed into ACA02 and ACA03 analog continuous time blocks. The amplifier output is routed through a internal PSoC Schmitt Trigger to input the first inverter, which has been placed into DCA04. The inverter output is connected to both piezoelectric crystal current bridge and the input of the second inverter, which has been placed in DCA05. The inverters form the bridge piezoelectric transmitter driver which allows for obtaining the maximum output power for the given supply voltage.

OBSOLETE

The sensor input signal is amplified by programmable gain amplifier (**PGA**) placed into ACA00 and is filtered by vertical band-pass filter placed into ASB13 and ASA23. The filter center frequency is selected to be at the piezoelectric transmitter resonant frequency. The maximum sample ratio is equal to 30, which is sufficient. The PGA output is connected externally with filter input; the PSoC routing and placement limitations prohibit making this connection internally. The programmable gain amplifier placed into ACA01 has been reconfigured as a zero-crossing detector by removing the operational amplifier feedback. For applications that demand an accurate spectrum analysis of Doppler-Effect signal, the **PGA** can be used directly by removing re-configuration code in software sources.

The mixer is combined with switched-capacitor low-pass filter **LPF$_1$**, which has been placed into ASA10 and ASB11 blocks. The amplitude modulation possibility of ASA10 block is used for the mixer operation. The mixer reference signal is brought in by way of *Global Output Bus 4* from the resonant generator. The filter output signal is routed by way of internal buffer to **P0[5]** port for debugging and testing purposes. Note that the LPF$_1$ filter cut-off frequency is selected to be 1200 Hz and the maximum sample ratio is near 140 for good suppression of ultrasound-carrier conversion high-frequency products.

The **LPF$_1$** filter output signal is sampled by the 8-bit sigma delta **ADC$_1$** and the subsequent processing is being done in software. The sigma-delta ADC selection is based on low CPU overheads and good AC characteristics. The **ADC$_1$** sample rate is 2.6 kHz. To measure the reflected signal level, the incremental 12-bit ADC is used. The ADC conversion time is the longest among other ADC types for given clock frequency, which allows effective suppressing of the unwanted reflected signal amplitude modulation. In our case, **ADC$_2$** sample rate is near 40 Hz.

The timer placed into DBA03 forms the baud rate signal serial transmitter that has been placed into DCA06. The **ADC$_1$** data stream can be passed via COM port to a PC for analysis or processing in sensor-alternative applications.

Sensor Firmware

The sensor analyzes the Doppler-Effect signal continuously and turns on the alarm if the value of this signal within the inspected frequency range is bigger than some threshold value. The sensor software is implemented using the interrupt-main loop programming technique. The real-time data collection and processing algorithms are implemented in the **ADC$_1$** interrupt routine. Analysis of reflected signal level and sending the **ADC$_1$** data stream are implemented in the main software loop. The software sources allow building two software versions; debug and release dependent on the *DEBUG* variable definition. The debug software version sends the **ADC$_1$** filtered data stream via the serial transmitter together with other debug information. In the release version, these features are omitted which reduces power consumption and saves code space.

The main loop is quite simple. After reset, peripheral devices are initiated and data collection is started. Then, the level measuring **ADC$_2$** samples the sensors and updates the low-level LED status. Finally, the **ADC$_1$** sample status is checked and sent via serial port, if the debug software version has been built.

The data processing algorithms are implemented in the **ADC$_1$** interrupt routine. First, the low-pass filtering is performed for removing the high-frequency noise from Doppler-Effect signal. Next, the low-pass filter output data stream is directed to the high-pass filter to remove the lower frequency spectrum portion, which is done to improve the sensor noise resistance. Lastly, the amplitude analysis of the high-pass filter output is performed to detect the alarm signals. The alarm is turned on when the predefined number of interrupt cycles of the alarm condition has been detected.

The digital filters are implemented as finite impulse response (FIR) filters using the PSoC MCU multiple-accumulation unit (MAC). The low-pass filter operates at the **ADC$_1$** sample rate, and the filter cut-off frequency is set near 300 Hz. The filter length was selected to 11 taps. The high-pass filter operates at a quarter of the ADC sample rate with cut-off frequency of approximately 20 Hz. The filter length was chosen to 15 taps for reliable operation under indoor and outdoor conditions, but could be reduced to 7 in a less noisy environment.

The corresponding conditional compilation variable, **BPF_HIGH**, is present in the software source. Note that the lower sample rate of the FIR **HPF** was selected to provide the low cut-off frequency with smaller number of filter taps. Because the high-pass filter operates at a quarter sample rate, the Interrupt Service Routine (ISR) structure was optimized to provide balancing of CPU resources.

CYPRESS PROPRIETARY

Because the high-pass filter operates with a lower sample rate, the **LPF_2** output does not require sampling on every interrupt. So, in the first interrupt time we calculate the **LPF_2** sample, next process this sample via digital **HPF** and perform the **HPF** output analysis in third interrupt routine call. Note that the **LPF_2** circular buffer must be updated each time. Figure 6 illustrates the proposed algorithm:

Figure 6. Data Processing Interrupt Routine Structure

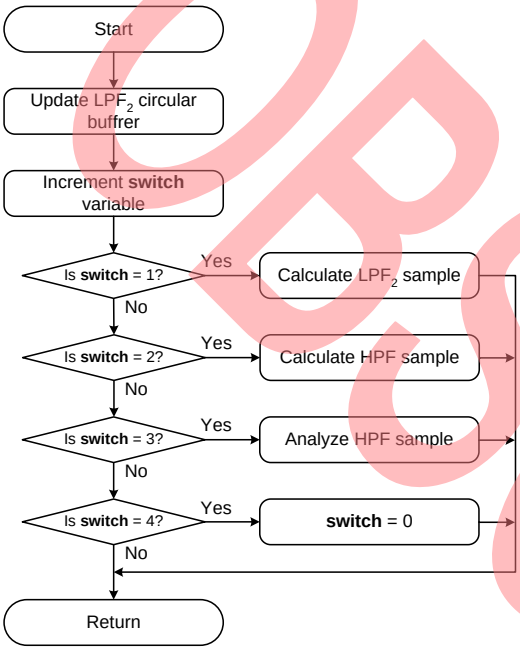

To detect alarm events, a software peak detector has been implemented. Alternatively, a true RMS detector can be easily implemented using the PSoC MAC. No difference between these two approaches was observed.

The current version of the sensor firmware is relatively simple. It consumes only 3 Kbytes of code and 60 bytes of data RAM. The rest of the code and data memory is at user disposal and can be used for embedding the proposed sensor into various applications. For example, the author has combined this sensor with a doorbell for automatic sound level and melody changing when anyone comes close to the home entrance door. The PSoC MCU dynamic reconfiguration possibility allows on-the-fly dynamic changing of PSoC functions and use of previously allocated hardware resources for alternative purposes.

The current software release was written in ‘C’ and runs at 12 MHz. It is expected that assembly level optimization will allow the decrease of the CPU clock frequency two or more times for additional reduction in power consumption.

Design Variances and Sensor’s Alternative Applications

The proposed sensor hardware and software were optimized for security system applications. For some types of these applications, the obtained operation range is unacceptable. For achieving larger operational distances, combine an external-power amplifier with a low-noise preamplifier. The standard MOSFET driver is ideally suitable for piezoelectric sensor driving because it is intended to drive large capacitance loads. The preamplifier will amplify the low-level signals. Figure 7 depicts the proposed schematic of this unit. The proposed amplifier is characterized by a maximum gain on the piezoelectric sensor resonant frequency, which allows suppression of the off-band noise signals.

OBSOLETE

Figure 7. External Amplifiers for Longer Operational Range

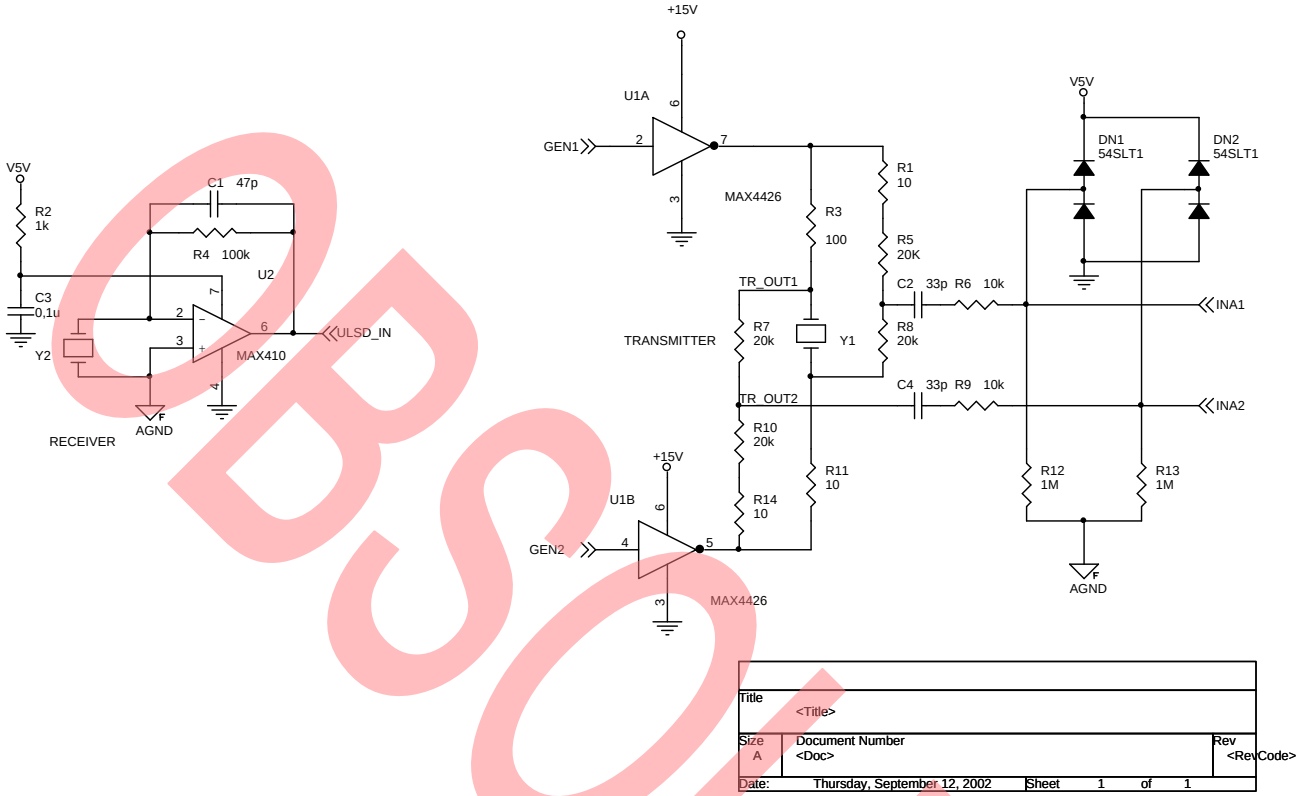

OBSOLETE

For the resonant generator variants, the PSoC MCU internal Schmitt Trigger is used for converting the amplifier analog signal into digital. Alternatively, the signal from *Comparator Bus 2* can be routed to *Global Output Bus 5* via the SPIS User Module.

Note SPIS is a non-inverting module, so the signal must be first routed to Global Output Bus 5 and later to Global Output Bus 4 via digital inverter to preserve existing sensor schematic.

This approach has been tested but larger power consumption and jitter on generated waveform has been observed.

The scope of sensor applications is not limited to security systems. These applications can be used for such products as movement-activated intellectual children toys, automatic door opening systems, and identification systems. Also, the sensor can be used for remote, contact-less speed measurement and machined parts-vibration analysis. For example, the sensor can be built into various sports training equipment for controlling the practice pace and optimizing the training load time distribution.

For speed measurement applications, the speed can be determined by measuring the frequency of the Doppler-Effect signal. The methods that can be used include the “classic” counter frequency/period measuring method, FFT or correlation technique, wavelet transformation-based analysis, and so on. The wavelet transformation is optimal for analyzing non-stationary signals.

Figure 8. Doppler-Effect Signal Example Time Graph (a); its FFT (b)

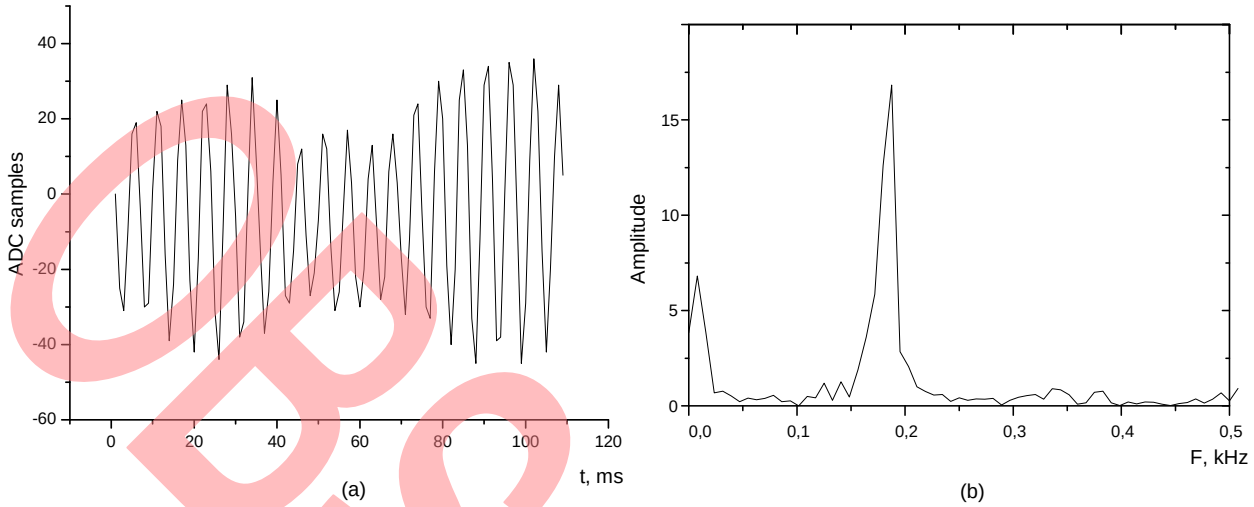

OBSOLETE

Summary

The ultrasound motion detection sensor has been presented. The sensor can be used for building various intelligent devices, including home, office and car security systems, intellectual toys, and home appliances. The software sources, schematics, and board layout reference design simplify sensor adaptation for concrete application demands. The associated project includes full schematic and board layout files in Cadence Orcad 9.2. Note that the layout was performed for components on hand. Using smaller footprint components will allow you to build the sensor with noticeably smaller dimensions.

About the Author

Name: Victor Kremin.

OBSOLETE

Appendix A

Figure 9. Component Placement Layer and Board Layout Layers, Actual Size

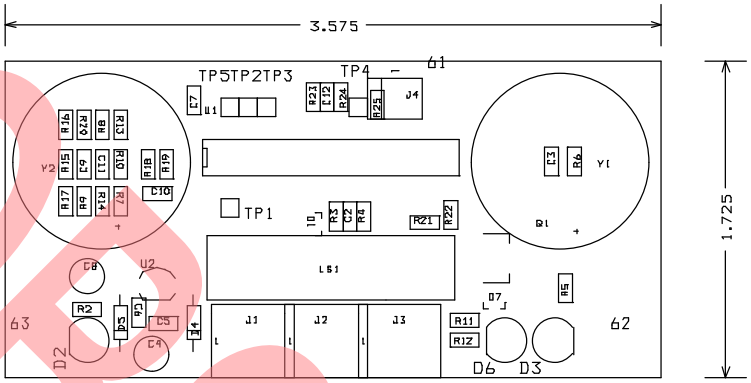

Component labels (dimensions are in inches)

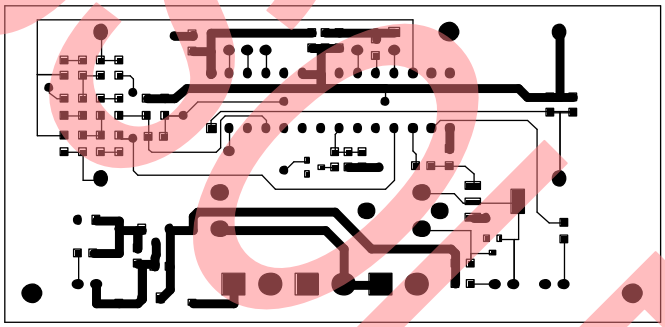

Top layout layer

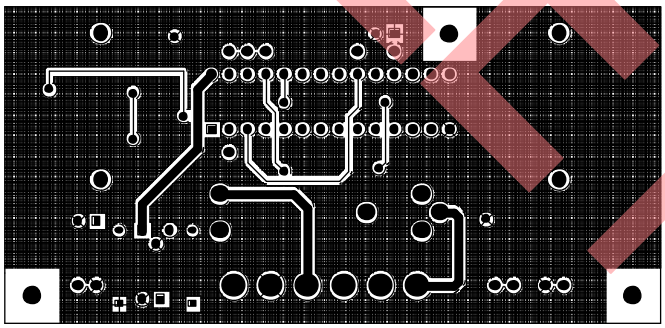

Bottom layout layer

OBSOLETE

Figure 10. Sensor Photograph, Actual Size

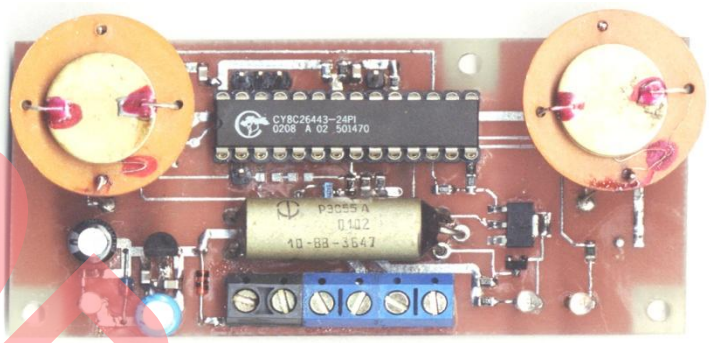

OBSOLETE

Document History

Document Title: Sensing: Ultrasound Motion Sensor - AN2047

Document Number: 001-40920

Revision	ECN	Orig. of Change	Submission Date	Description of Change
**	1536344	XSG	10/03/2007	OLD APP. NOTE: Obtained spec # for note to be added to spec system.
*A	3197863	BIOL	03/16/2011	Updated BOOT.TPL file. Updated UM versions.
*B	4348867	GRAA	04/16/2014	Updated in new template. Completing Sunset Review.
*C	4748548	GRAA	04/30/2015	Obsolete document. Completing Sunset Review.

OBSOLETE

Worldwide Sales and Design Support

Cypress maintains a worldwide network of offices, solution centers, manufacturer's representatives, and distributors. To find the office closest to you, visit us at Cypress Locations.

Products

Automotive	cypress.com/go/automotive
Clocks & Buffers	cypress.com/go/clocks
Interface	cypress.com/go/interface
Lighting & Power Control	cypress.com/go/powerpsoc cypress.com/go/plc
Memory	cypress.com/go/memory
PSoC	cypress.com/go/psoc
Touch Sensing	cypress.com/go/touch
USB Controllers	cypress.com/go/usb
Wireless/RF	cypress.com/go/wireless

PSoC® Solutions

psoc.cypress.com/solutions

PSoC 1 | PSoC 3 | PSoC 4 | PSoC 5LP

Cypress Developer Community

Community | Forums | Blogs | Video | Training

Technical Support

cypress.com/go/support

OBSOLETE

PSoC is a registered trademark of Cypress Semiconductor Corp. "Programmable System-on-Chip," PSoC Designer, and PSoC Express are trademarks of Cypress Semiconductor Corp. All other trademarks or registered trademarks referenced herein are the property of their respective owners.

Cypress Semiconductor
198 Champion Court
San Jose, CA 95134-1709

Phone : 408-943-2600
Fax : 408-943-4730
Website : www.cypress.com

© Cypress Semiconductor Corporation, 2007-2015. The information contained herein is subject to change without notice. Cypress Semiconductor Corporation assumes no responsibility for the use of any circuitry other than circuitry embodied in a Cypress product. Nor does it convey or imply any license under patent or other rights. Cypress products are not warranted nor intended to be used for medical, life support, life saving, critical control or safety applications, unless pursuant to an express written agreement with Cypress. Furthermore, Cypress does not authorize its products for use as critical components in life-support systems where a malfunction or failure may reasonably be expected to result in significant injury to the user. The inclusion of Cypress products in life-support systems application implies that the manufacturer assumes all risk of such use and in doing so indemnifies Cypress against all charges.

This Source Code (software and/or firmware) is owned by Cypress Semiconductor Corporation (Cypress) and is protected by and subject to worldwide patent protection (United States and foreign), United States copyright laws and international treaty provisions. Cypress hereby grants to licensee a personal, non-exclusive, non-transferable license to copy, use, modify, create derivative works of, and compile the Cypress Source Code and derivative works for the sole purpose of creating custom software and or firmware in support of licensee product to be used only in conjunction with a Cypress integrated circuit as specified in the applicable agreement. Any reproduction, modification, translation, compilation, or representation of this Source Code except as specified above is prohibited without the express written permission of Cypress.

Disclaimer: CYPRESS MAKES NO WARRANTY OF ANY KIND, EXPRESS OR IMPLIED, WITH REGARD TO THIS MATERIAL, INCLUDING, BUT NOT LIMITED TO, THE IMPLIED WARRANTIES OF MERCHANTABILITY AND FITNESS FOR A PARTICULAR PURPOSE. Cypress reserves the right to make changes without further notice to the materials described herein. Cypress does not assume any liability arising out of the application or use of any product or circuit described herein. Cypress does not authorize its products for use as critical components in life-support systems where a malfunction or failure may reasonably be expected to result in significant injury to the user. The inclusion of Cypress' product in a life-support systems application implies that the manufacturer assumes all risk of such use and in doing so indemnifies Cypress against all charges.

Use may be limited by and subject to the applicable Cypress software license agreement.